© 2017. Published by The Company of Biologists Ltd | Journal of Cell Science (2017) 130, 2914-2925 doi:10.1242/jcs.204842

RESEARCH ARTICLE

Ezrin directly interacts with AQP2 and promotes its endocytosis

Wei Li[1], William W. Jin[2], Kenji Tsuji[1], Ying Chen[1], Naohiro Nomura[1,*], Limin Su[1,3], Naofumi Yui[1,*], Julian Arthur[1,‡], Susanna Cotecchia[4], Teodor G. Păunescu[1], Dennis Brown[1] and Hua A. J. Lu[1,§]

ABSTRACT

The water channel aquaporin-2 (AQP2) is a major regulator of water homeostasis in response to vasopressin (VP). Dynamic trafficking of AQP2 relies on its close interaction with trafficking machinery proteins and the actin cytoskeleton. Here, we report the identification of ezrin, an actin-binding protein from the ezrin/radixin/moesin (ERM) family as an AQP2-interacting protein. Ezrin was first detected in a co-immunoprecipitation (co-IP) complex using an anti-AQP2 antibody in a proteomic analysis. Immunofluorescence staining revealed the co-expression of ezrin and AQP2 in collecting duct principal cells, and VP treatment caused redistribution of both proteins to the apical membrane. The ezrin–AQP2 interaction was confirmed by co-IP experiments with an anti-ezrin antibody, and by pulldown assays using purified full-length and FERM domain-containing recombinant ezrin. By using purified recombinant proteins, we showed that ezrin directly interacts with AQP2 C-terminus through its N-terminal FERM domain. Knocking down ezrin expression with shRNA resulted in increased membrane accumulation of AQP2 and reduced AQP2 endocytosis. Therefore, through direct interaction with AQP2, ezrin facilitates AQP2 endocytosis, thus linking the dynamic actin cytoskeleton network with AQP2 trafficking.

KEY WORDS: Aquaporin-2, Ezrin, Endocytosis, Trafficking, Water homeostasis

INTRODUCTION

AQP2 is a water channel that is expressed in the principal cells of kidney collecting ducts. It is the major channel that regulates water transport in response to vasopressin (VP), the antidiuretic hormone, which is secreted by the posterior pituitary in response to hyperosmolality and hypovolemia (Brown and Fenton, 2015). Circulating VP binds to vasopressin receptor 2 (V2R, also known as AVPR2) on principal cells, leading to activation of adenylyl cyclase, and elevation of intracellular cyclic AMP (cAMP). Elevated cAMP activates protein kinase A (PKA), which in turn phosphorylates AQP2 and causes AQP2 accumulation on the plasma membrane, thus increasing its water permeability and allowing transepithelial water flow. After VP withdrawal, AQP2 is endocytosed via clathrin-mediated endocytosis, and then proceeds to recycling and/or degradation pathways depending on the physiological context. In addition to the regulated trafficking events that are mediated by VP and cAMP or cGMP, AQP2 also undergoes constitutive recycling, which is independent of the VP/cAMP/phosphorylation cascade (Brown and Fenton, 2015).

The cortical cytoskeleton of eukaryotic cells not only provides structural support for the plasma membrane but also contributes to many dynamic processes such as endocytosis, exocytosis and transmembrane signaling events. Coordination between actin polymerization and depolymerization plays a key role in AQP2 trafficking, and actin depolymerization has long been associated with vasopressin stimulation of target cells (Hays et al., 1993). Furthermore, apical membrane accumulation of AQP2 can be induced by RhoA inactivation and actin depolymerization in the absence of VP stimulation (Klussmann et al., 2001; Tamma et al., 2001, 2003). We and others have also shown that statins cause membrane accumulation of AQP2 in cultured cells and increase urinary concentration in animals via their inhibitory effect on RhoA activity (Li et al., 2011; Procino et al., 2011).

The ezrin/radixin/moesin (ERM) proteins are a unique family that serve as crosslinkers between the plasma membrane and the actin cytoskeleton network. The ERM family contains several highly similar proteins including ezrin, moesin and radixin. Ezrin was the first protein identified and is also the best studied of the ERM family (Bretscher, 1983; Hunter and Cooper, 1981). Ezrin and other ERM proteins crosslink actin filaments with the plasma membrane, and play important structural and regulatory roles in the assembly and stabilization of specialized plasma membrane domains. In addition, they also act as signal transducers that mediate multiple signaling pathways including those involved in cell survival, proliferation, adhesion and migration in a variety of cell types (Berryman et al., 1993; Parameswaran et al., 2011). In addition, ERM proteins are also involved in membrane protein and vesicle trafficking (McClatchey and Fehon, 2009). For example, ERM proteins regulate trafficking of the α1β-adrenergic receptor NHE3 (also known as SLC9A3), the H^+-K^+-ATPase and other membrane transporters (Cha et al., 2006; Stanasila et al., 2006; Zhao et al., 2004; Zhou et al., 2005).

ERM proteins including ezrin have three functional domains: an N-terminal FERM domain (which is a widespread protein module shared by four-point one, ezrin, radixin and moesin proteins), an extended coiled-coil region that is rich in α-helices, and a short C-terminal domain containing a highly conserved F-actin-binding site and a highly conserved tyrosine residue, T567 (Gary and Bretscher, 1995; Turunen et al., 1994). The FERM domain is highly conserved and shares more than 85% similarity among ezrin, moesin

[1]Center for Systems Biology, Program in Membrane Biology and Division of Nephrology, Massachusetts General Hospital, and Harvard Medical School, Boston, MA 02114, USA. [2]Washington University in St. Louis, College of Arts and Sciences, St Louis, MO 63130, USA. [3]Department of Pharmacology, School of Basic Medical Sciences, Peking University, Beijing 100191, China. [4]Department of Pharmacology and Toxicology, University of Lausanne, Lausanne 1005, Switzerland.
*Present address: Tokyo Medical and Dental University, Graduate School of Medical and Dental Sciences, Tokyo, Japan. ‡Present address: Cell Signaling Technology, Danvers, MA, USA.

§Author for correspondence (Lu.Hua@mgh.harvard.edu)

W.L., 0000-0002-9025-7293; K.T., 0000-0001-5442-7008; Y.C., 0000-0002-6862-5678; L.S., 0000-0002-9863-863X; J.A., 0000-0003-1355-0960; H.A.J.L., 0000-0003-0553-6499

Received 13 April 2017; Accepted 21 July 2017

Journal of Cell Science

Journal of Cell Science (2017) 130, 2914-2925 doi:10.1242/jcs.204842

and radixin. It mediates both direct and indirect interactions with numerous membrane and membrane-associated proteins (Yonemura et al., 1999). A diverse group of membrane proteins have been shown to directly interact with ERM proteins including the hyaluronic acid receptor CD44, intercellular adhesion molecule (ICAM)-2, ICAM-3, syndecan 2 and the α1β-adrenergic receptor (Granés et al., 2000; Helander et al., 1996; Scholl et al., 1999; Serrador et al., 1997; Stanasila et al., 2006; Tsukita et al., 1994). In addition, ERM proteins also interact with multiple membrane proteins indirectly via adaptor proteins, such as EBP50 (also known as SLC9A3R1) (Donowitz et al., 2005; Reczek et al., 1997; Reczek and Bretscher, 1998).

We initially identified ezrin as an AQP2-interacting protein via mass spectrometry analysis of the co-IP complex generated using an anti-AQP2 antibody. Here, we confirmed and examined this interaction by performing multiple *in vitro* binding assays. A direct interaction of the ezrin FERM domain and the AQP2 C-terminus was indicated by pulldown assays using purified recombinant proteins. Knocking down ezrin expression in cells leads to membrane accumulation of AQP2, probably due to reduced AQP2 endocytosis. Our data therefore reveal that a direct interaction between ezrin and AQP2 plays an important role in mediating AQP2 trafficking and regulating its membrane accumulation.

RESULTS

Partial colocalization of ezrin and AQP2 on the apical membrane after VP treatment of MDCK cells

The distribution of ezrin and AQP2 in cells was examined using immunofluorescence staining of filter-grown, polarized MDCK cells expressing AQP2, in the presence or absence of VP stimulation. The immunofluorescence staining of ezrin was mainly detected in the basolateral region and cytosol, and AQP2 staining was mainly located in the subapical region under non-stimulated conditions (Fig. 1A, upper panels). After treatment with VP, the ezrin signal was redistributed to the apical membrane concomitantly with apical redistribution of AQP2 staining, presenting as a partial colocalization of ezrin and AQP2

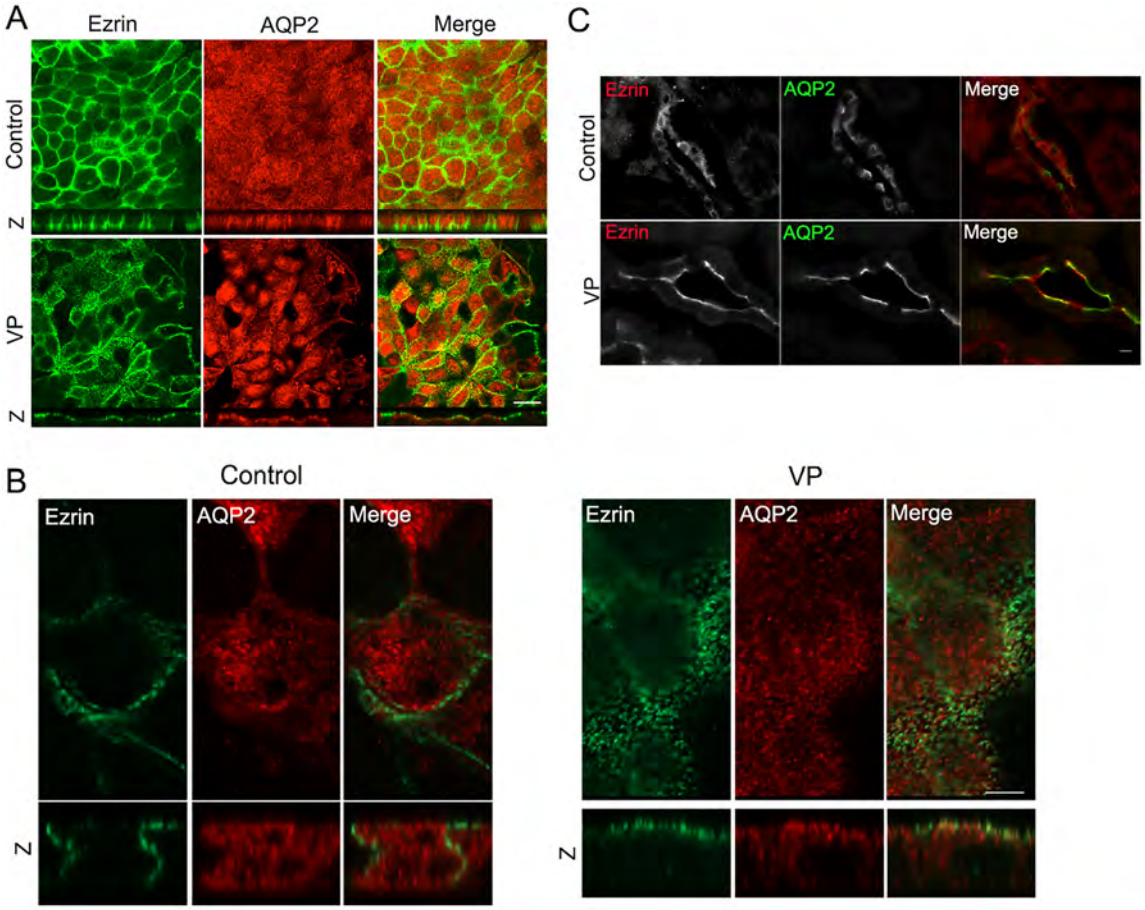

Fig. 1. VP treatment enhances apical AQP2 expression and its colocalization with ezrin. (A) VP treatment enhances apical AQP2 expression and its colocalization with ezrin in cultured renal epithelial cells. AQP2-MDCK cells were stained with antibodies against ezrin (green) and AQP2 (red) in the presence (VP) and absence (Control) of VP treatment (AVP 20 nM for 20 min). The larger panels represent confocal sections through the subapical regions of the cells above the nucleus. The smaller horizontal strips at the bottom of each panel are *z*-sections through the entire cell for direct comparison of the respective staining intensities of the apical and basolateral membranes, and the cytosol. Upper panels show that in the absence of VP stimulation, ezrin staining localized to the cytosol and basolateral region, while AQP2 staining was mainly detected in the subapical region. Lower panels show that after VP treatment, the ezrin signal was redistributed toward the apical and sub-apical regions and partially colocalized with the similarly apically redistributed AQP2. Scale bar: 10 µm. (B) Super-resolution Airyscan confocal microscopy imaging revealed that AQP2 and ezrin partially colocalize on the apical membrane in VP-treated MDCK cells. Left panels show no apparent colocalization of ezrin and AQP2, in the absence of VP stimulation. Right panels are cells treated with VP. Scale bar: 5 µm. (C) AQP2 and ezrin are co-expressed in principal cells of the Brattleboro rat collecting duct, and co-accumulate on the plasma membrane after vasopressin treatment. Without VP treatment (Control), ezrin was located in the cytosol and basal region, while AQP2 was detected mainly in the sub-apical region of the principal cells of the collecting ducts. After 7 days of VP treatment (VP), ezrin (red in the merge panel) colocalized with AQP2 (green in the merge panel) on the plasma membrane of the principal cells. Scale bar: 20 µm.

Journal of Cell Science (2017) 130, 2914-2925 doi:10.1242/jcs.204842

immunofluorescence signals on the apical membrane in response to VP (Fig. 1A, lower panels and *z*-plane). High-resolution imaging of filter-grown polarized MDCK cells was performed using a Zeiss LSM800 confocal microscope with Airyscan capability (Carl Zeiss, Jena, Germany). The Airyscan imaging confirmed the partial colocalization of ezrin and AQP2 on the apical membrane upon VP treatment (Fig. 1B, right panels and *z*-plane). Therefore, VP treatment enhances apical expression of ezrin and increases its apical colocalization with AQP2 in polarized MDCK cells.

Colocalization of ezrin and AQP2 on the apical plasma membrane of principal cells in VP-treated Brattleboro rats

Immunofluorescence staining with anti-ezrin and anti-AQP2 antibodies was performed in kidney tissues from Brattleboro rats in the presence or absence of VP treatment (Fig. 1C). Without VP treatment, ezrin staining was located mainly in the cytosol, subapical and basal regions, while AQP2 staining was located in the subapical and basolateral region in the majority of principal cells in the collecting ducts (Fig. 1C, upper panels). After 7 days of VP treatment, the ezrin signal redistributed towards the apical and subapical regions and away from the basal region, while AQP2 accumulated prominently on the apical plasma membrane, as expected (Nielsen et al., 1997; Sabolić et al., 1995). Partial colocalization of ezrin and AQP2 signals was seen at the apical plasma membrane of collecting duct principal cells in VP-treated animals (Fig. 1C, lower panels).

Interaction of AQP2 and ezrin is detected in a co-IP assay

A possible physical interaction of AQP2 and ezrin was first suggested by the mass spectrometry analysis of a co-IP complex from mouse kidney lysate performed using an anti-AQP2 antibody (Fig. 2A). Mass spectrometry data revealed multiple ezrin peptides in the co-IP complex when using antibodies against wild-type AQP2 and AQP2 phosphorylated at serine 256. No ezrin peptides were detected in the co-IP complex, when using antibodies specific to AQP2 phosphorylated at serine 261, 269 or 264. The interaction of ezrin and AQP2 was then examined in an *in vitro* co-IP assay (Fig. 2B,C). Using a rabbit anti-ezrin antibody (Fig. 2B), we were able to detect AQP2 in the co-IP complex from both mouse kidney and AQP2-expressing cultured cell lysates. Similarly, a co-IP experiment using a rabbit anti-AQP2 antibody was performed (Fig. 2C), and we were able to detect ezrin in the co-IP complex from both mouse kidney and AQP2-expressing cultured cell lysates. We also performed a co-IP experiment using rabbit IgG to exclude the possibility of non-specific binding, and detected no ezrin or AQP2 in the co-IP complex from both lysates (data not shown). It was important to ensure that both the cell and tissue lysate used for co-IP were solubilized, without including large insoluble membrane/vesicle components (see Materials and Methods) because false interactions may occur when two proteins are present in the same membrane domain under these conditions, even in the absence of an actual direct interaction between them.

The N-terminal FERM domain of ezrin is necessary for interaction with AQP2

To further confirm the interaction between AQP2 and ezrin, and identify the possible AQP2-interacting domain of ezrin, we performed pulldown experiments using histidine (His)-tagged recombinant ezrin protein (Fig. 3). His-tagged recombinant ezrin constructs of various functional regions were previously

A

Beads	Anti-AQP2	Anti-pS256-AQP2	Anti-pS261-AQP2	Anti-pS269-AQP2	Anti-pS264-AQP2
×	APDFVFYAPR IGFPWSEIR VSAQEVR	APDFVFYAPR RKPDTIEVQQMK SQEQLAAELAEYTAK IGFPWSEIR VSAQEVR ALQLEEERR	×	×	×

×: Not detected,
Antibodies used for co-IP are: anti-total AQP2 antibody, and AQP2 phosphorylation specific antibodies for serine 256, serine 261, serine 264, and serine 269.

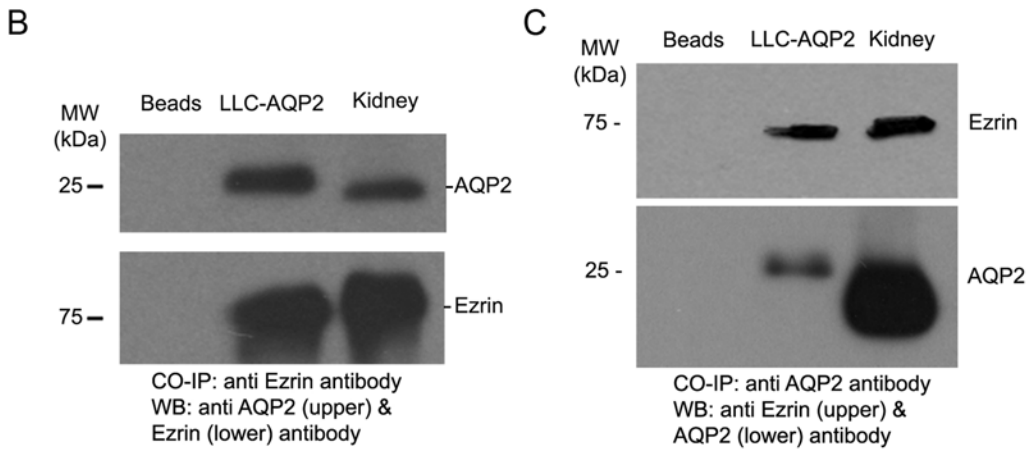

Fig. 2. Interaction of AQP2 with ezrin is detected in co-IP experiments. (A) List of ezrin peptides detected by mass spectrometry from the AQP2 co-IP complex. (B,C) By using an anti-ezrin antibody for co-IP, we were able to detect AQP2 in the co-IP complex from stable AQP2-expressing LLC-PK1 cell lysates and mouse kidney (B). Similarly, ezrin signal was detected in the co-IP complex using anti-AQP2 antibody (C). WB, western blotting.

Journal of Cell Science (2017) 130, 2914-2925 doi:10.1242/jcs.204842

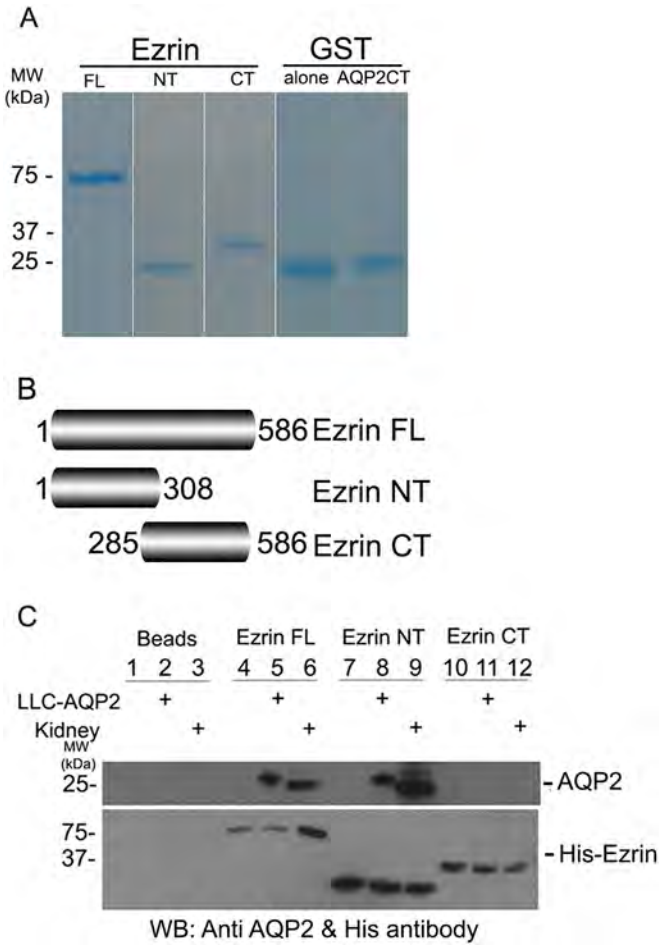

Fig. 3. AQP2 interacts with ezrin via the ezrin N-terminal FERM-containing domain. (A) Recombinant His-tagged ezrin full-length (FL, amino acids 1–586), N-terminus (NT, amino acids 1–308), and C-terminus (CT, amino acids 285–586) were expressed in *E. coli* and purified to homogeneity as revealed by SDS-PAGE together with purified recombinant AQP2 C-terminus (AQP2CT). Schematic representation of each recombinant protein is shown in B. (C) The purified His-tagged ezrin full-length protein (FL) and the N-terminal FERM-containing recombinant protein (but not the C-terminal protein) were able to pull down AQP2 from both LLC-AQP2 cell lysates and mouse kidney lysates. Lanes 1–3, beads alone pulled down with PBS (lane 1), LLC-AQP2 cell lysate (lane 2) and kidney lysate (lane 3); lanes 4–6, ezrin FL pulled down with PBS (lane 4), LLC-AQP2 cell lysate (lane 5) and kidney lysate (lane 6); lanes 7–9, ezrin NT pulled down with PBS (lane 7), LLC-AQP2 cell lysate (lane 8) and kidney lysate (lane 9); lanes 10–12, ezrin CT pulled down with PBS (lane 10), LLC-AQP2 cell lysate (lane 11) and kidney lysate (lane 12). WB, western blotting.

characterized (Stanasila et al., 2006). These ezrin constructs include full-length ezrin, the N-terminal region of ezrin, which contains the FERM domain and a C-terminal region of ezrin, which contains the actin-binding site and a key phosphorylation site (T567). A schematic representation of the recombinant ezrin constructs is shown in Fig. 3B. The recombinant His-tagged full-length, N-terminus and C-terminus ezrin were expressed in *E. coli*, were of the predicted molecular mass, and were purified to homogeneity as shown by Coomassie Blue staining after SDS-PAGE (Fig. 3A). Pulldown experiments revealed that both the purified full-length ezrin recombinant protein and the FERM domain-containing N-terminal ezrin recombinant protein were able to pull down AQP2 from AQP2-expressing cells and mouse kidney lysates, while the C-terminus recombinant ezrin protein failed to pull down AQP2 (Fig. 3C). These data suggest that ezrin interacts with AQP2 through its N-terminal FERM domain, as is the case for its direct and indirect interactions with many other membrane proteins (Donowitz et al., 2005; Granés et al., 2000; Reczek et al., 1997; Reczek and Bretscher, 1998; Stanasila et al., 2006).

Ezrin directly interacts with AQP2 C-terminus through its N-terminal FERM domain

We next investigated whether the interaction of AQP2 with ezrin FERM domain is direct or indirect, in a pulldown experiment using purified recombinant ezrin and AQP2 proteins. The AQP2 C-terminus has been shown to contain multiple key regulatory elements and is believed to be critical for AQP2 trafficking and regulation. We, along with Dr. Knepper's group, have previously shown that heat shock protein 70 (Hsc70 or Hsp70) directly interacts with the C-terminus of AQP2 and mediates AQP2 trafficking (Lu et al., 2007; Zwang et al., 2009). Therefore, we now focused on a possible interaction of the ezrin FERM domain and the AQP2 C-terminus. A recombinant, GST-tagged AQP2 C-terminus protein was expressed in *E. coli* and purified to homogeneity as shown by SDS-PAGE (Fig. 3A). The purified His-tagged full-length ezrin protein, and its N- and C-terminus were used to pull down the purified GST-tagged AQP2 C-terminus protein. Both the purified full-length and N-terminus ezrin were able to pull down the purified AQP2 C-terminus, while the purified ezrin C-terminus failed to do so (Fig. 4). These data show that the interaction of AQP2 and ezrin is a direct physical interaction, and occurs between the ezrin FERM domain and the AQP2 C-terminus.

Downregulation of ezrin causes membrane accumulation of AQP2 independently of VP stimulation

The function of ezrin in AQP2 trafficking was next examined in cultured cells in which endogenous ezrin expression was knocked down using shRNA (Fig. 5). Immunoblots revealed a large, almost 80%, reduction of the endogenous ezrin in LLC-AQP2 cells transfected with ezrin shRNA for 48 h in comparison to mock-transfected cells, while no significant change of total AQP2 was detected (Fig. 5A). After knocking down ezrin in LLC-AQP2 cells, a significant membrane accumulation of AQP2 was detected under baseline conditions, similar to that seen in VP-treated cells (Fig. 5B). Membrane accumulation of AQP2 after

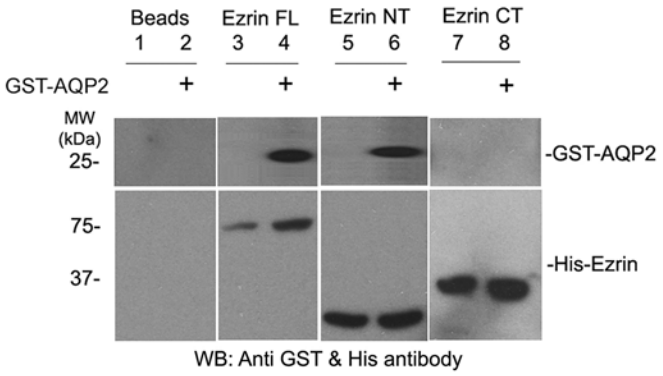

Fig. 4. AQP2 C-terminus directly interacts with ezrin N-terminal FERM-containing domain. The direct interaction of AQP2 and ezrin is revealed by pulldown experiments using purified recombinant ezrin and AQP2 proteins. Only the purified ezrin full-length (FL) and the N-terminus FERM domain-containing (NT) recombinant protein were able to pull down the purified AQP2 C-terminus. The ezrin C-terminal domain (CT) did not pull down the AQP2 C-terminal domain. WB, western blotting.

Journal of Cell Science (2017) 130, 2914-2925 doi:10.1242/jcs.204842

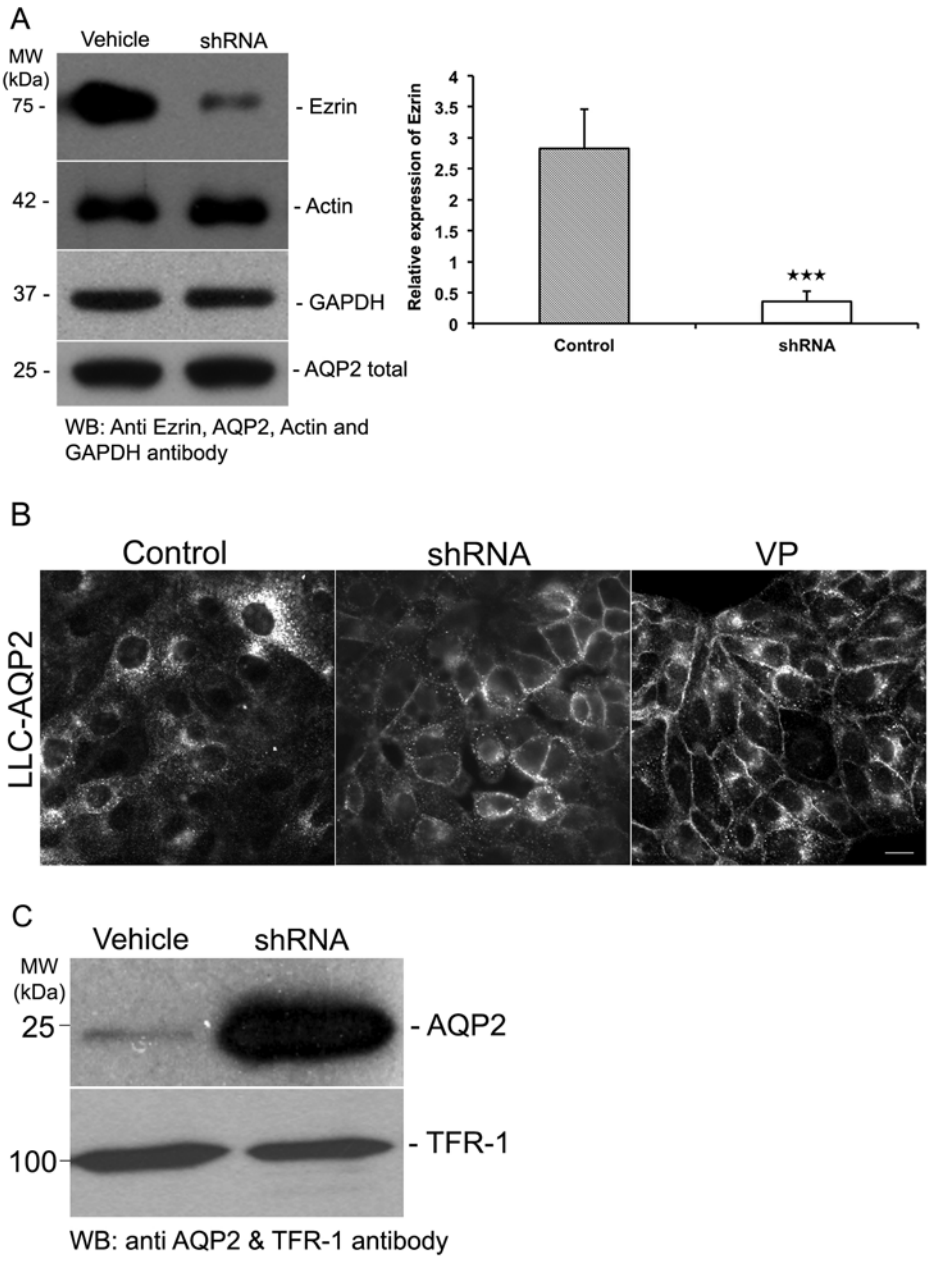

Fig. 5. Downregulating ezrin causes membrane accumulation of AQP2. (A) Immunoblotting revealed a strong knockdown of endogenous ezrin in LLC-AQP2 cells by ezrin shRNA lentivirus. There was an ∼80% reduction of endogenous ezrin in ezrin shRNA knockdown LLC-AQP2 cells (graph shows the quantification of ezrin band intensity relative to actin). Results are mean±s.e.m. ($n \geq 3$). ***$P<0.001$ (one-way ANOVA). (B) Immunofluorescence staining of AQP2 in control LLC-AQP2 cells and cells infected with ezrin shRNA lentivirus. After knocking down ezrin in LLC-AQP2 cells, AQP2 was found to increasingly accumulate on the cell surface under baseline conditions (without any stimulation). VP-treated LLC-AQP2 cells were used for comparison. Scale bar: 10 µm. (C) Surface biotinylation experiment revealed a significantly increased accumulation of AQP2 signal on cell surface after knocking down ezrin expression in cells. Transferrin receptor 1 (TFR-1) was used as an internal control for stable membrane proteins. WB, western blotting.

knocking down ezrin was further confirmed by surface biotinylation experiments (Fig. 5C). A significant membrane accumulation of AQP2 was again detected as a strong band of biotinylated AQP2 signal pulled down by streptavidin in ezrin knockdown cells. The surface biotinylated transferrin receptor 1 (TFR-1; also known as TFRC) was used as control and reference of a steady-state membrane-resident protein (Fig. 5C). Both immunofluorescence staining and surface biotinylation experiments show that knocking down ezrin expression in LLC-AQP2 cells is sufficient to cause AQP2 membrane accumulation in the absence of VP stimulation.

Membrane accumulation of AQP2 induced by ezrin knockdown is independent of changes in AQP2 phosphorylation or cAMP elevation

In addition to organizing the actin cytoskeleton, ezrin also mediates signaling pathways. To understand whether ezrin affects AQP2 trafficking through modifying AQP2 phosphorylation, the phosphorylation state of AQP2 serine 256 and serine 261 was examined. Immunoblotting was performed using AQP2 phosphorylation-specific antibodies (Fig. 6A) as previously described (Rice et al., 2012). VP treatment caused increased phosphorylation of serine 256 and reduced phosphorylation of serine 261, which is consistent with previous reports (Rice et al., 2012). Knocking down ezrin in LLC-AQP2 cells did not alter the AQP2 phosphorylation at serine 256 or serine 261 (Fig. 6A). Therefore, the membrane accumulation of AQP2 induced by ezrin knockdown did not involve the altered phosphorylation of two key AQP2 residues.

Furthermore, knockdown of ezrin did not cause an elevation of intracellular cAMP as measured by a commercial cAMP ELISA assay, while in contrast, VP stimulation led to a significant increase of intracellular cAMP in cells as expected (Fig. 6B) (Yui et al., 2013). This suggests that AQP2 membrane accumulation induced by ezrin knockdown is not likely to involve the canonical VP-mediated signaling pathway.

Journal of Cell Science (2017) 130, 2914-2925 doi:10.1242/jcs.204842

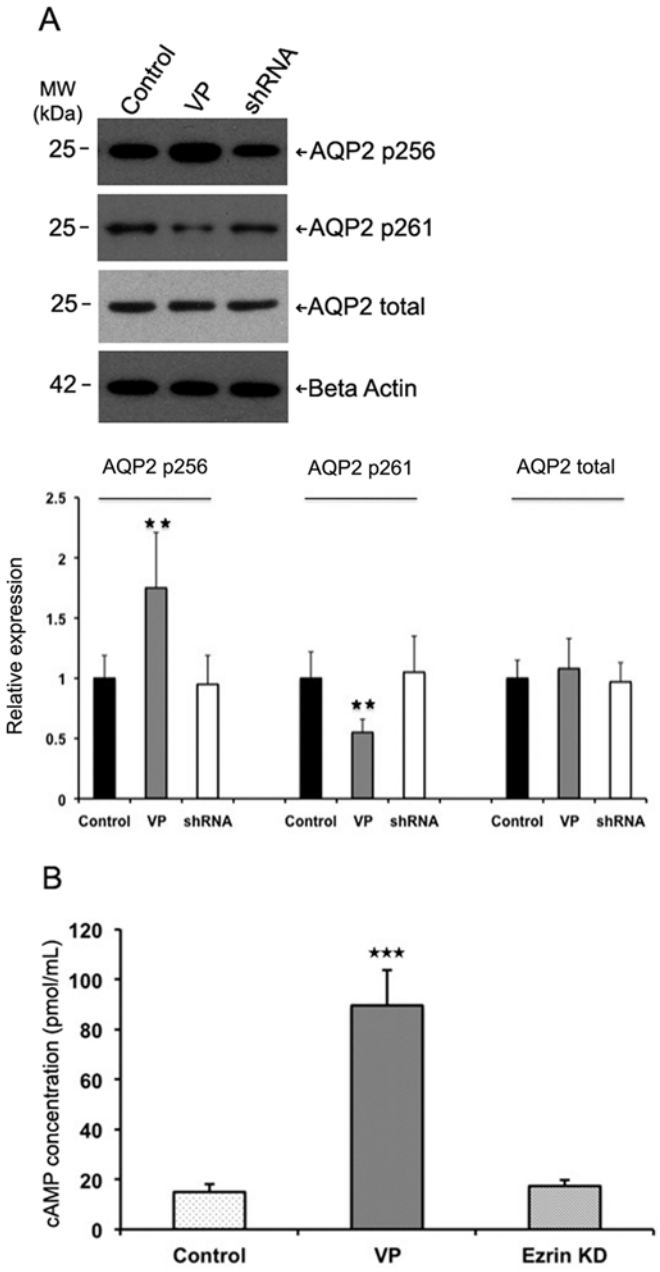

Fig. 6. Phosphorylation of key residues in AQP2 was not altered in ezrin knockdown cells. (A) Representative western blot showing that there is no alteration of the levels of total AQP2 and AQP2 phosphorylated at residues 256 or 261 in ezrin shRNA lentivirus-infected LLC-AQP2 cells unlike in cells treated with VP. Immunoblot using anti-β-actin antibody was used as control. Quantification of western blotting results for AQP2 phosphorylated on S256 (p256), S261 (p261) and total AQP2. (B) Intracellular cAMP measurement in LLC-PK1 cells. The intracellular cAMP concentration was significantly increased by 30 min VP treatment (20 nM LVP) without clonal variation. After ezrin knockdown no significant difference in cAMP concentration was observed compared to control. Results in A and B are mean±s.e.m. ($n \geq 3$). $^{**}P<0.01$, $^{***}P<0.001$ (one-way ANOVA).

Ezrin knockdown reduces clathrin-mediated endocytosis but does not affect overall exocytosis

Ezrin has been reported to be involved in both exocytosis and endocytosis of membrane proteins with which it associates (Stanasila et al., 2006). We next examined which AQP2 trafficking step was affected by ezrin, that is whether AQP2 membrane accumulation caused by knocking down ezrin was due to increased exocytosis, reduced endocytosis or both. We, therefore, performed exocytosis and endocytosis assays in the presence of ezrin knockdown in LLC-AQP2 cells.

Exocytosis was examined in LLC-AQP2 cells treated with ezrin shRNA, using our previously developed exocytosis assay (Nunes et al., 2008). LLC-AQP2 cells stably expressing soluble secreted yellow fluorescent protein (ssYFP) (LLC-AQP2-ssYFP cells) were generated for this exocytosis assay. ssYFP secreted into the extracellular medium was used as a surrogate marker for AQP2 exocytotic activity. Treating LLC-AQP2-ssYFP cells with VP resulted in a significant increase of ssYFP signal in the medium, indicating increased exocytosis of ssYFP by cells, which is consistent with previous reports (Nunes et al., 2008). Ezrin knockdown in LLC-AQP2-ssYFP cells did not increase the measured fluorescence signal in the extracellular medium in this assay. Therefore, ezrin knockdown had no significant impact on the overall exocytotic process in LLC-AQP2-ssYFP cells (Fig. 7A).

We then performed endocytosis assays. We have previously shown that AQP2 is endocytosed through a clathrin-mediated pathway (Sun et al., 2002). Consequently, we performed a clathrin-mediated endocytosis assay using fluorescent dye-conjugated transferrin. Methyl-β-cyclodextrin (MβCD), a cholesterol-chelating agent that has a very potent blocking effect on endocytosis (Lu et al., 2004; Rodal et al., 1999; Subtil et al., 1999) was used as positive control. Knocking down ezrin in LLC-AQP2 cells significantly reduced endocytosis of Alexa Fluor 568-conjugated transferrin. Interestingly, much of the fluorescent dye-conjugated transferrin was retained on the plasma membrane in both ezrin knockdown cells and cells treated with βCD (Fig. 7B upper panels). The fluorescence intensity of the internalized AlexaM Fluor 568–transferrin signal in control cells, ezrin knockdown cells and cells treated with MβCD was quantified and is shown in Fig. 7C. The extent of blockage of clathrin-mediated endocytosis by ezrin knockdown was comparable to that seen in cells treated with MβCD, suggesting a potent blocking effect of ezrin knockdown on endocytosis. Dual immunofluorescence staining for transferrin and AQP2 revealed discrete and strong membrane accumulation of AQP2 in the ezrin knockdown cells, as well as reduced transferrin uptake (Fig. 7B). Therefore, downregulation of ezrin caused apical membrane accumulation of AQP2 and a concomitant reduction of clathrin-mediated endocytosis.

Downregulation of ezrin reduces internalization of AQP2 in cells

It was observed many years ago that incubating cells at 20°C inhibited the exit of membrane proteins from the trans-Golgi network (TGN), thus blocking their transport to the plasma membrane (Griffiths et al., 1985). Instead, internalized membrane proteins accumulated in the perinuclear region, forming in time a so-called ‘perinuclear patch’ (Rice et al., 2012). In the absence of ongoing protein synthesis, the size and density of the perinuclear patch formed over time during the 20°C incubation reflects the rate of internalization of the membrane protein of interest (Rice et al., 2015). We have routinely used this ‘cold block’ assay to measure the rate of AQP2 internalization. A cold block experiment was performed in LLC-AQP2 cells after ezrin knockdown (Fig. 8). In control cells without ezrin knockdown, an AQP2 perinuclear patch started to form at ∼30 min after cold block, and the patch signal plateaued at ∼120 min. Conversely, in ezrin knockdown cells the AQP2 signal was mostly retained at the plasma membrane for up to

Journal of Cell Science (2017) 130, 2914-2925 doi:10.1242/jcs.204842

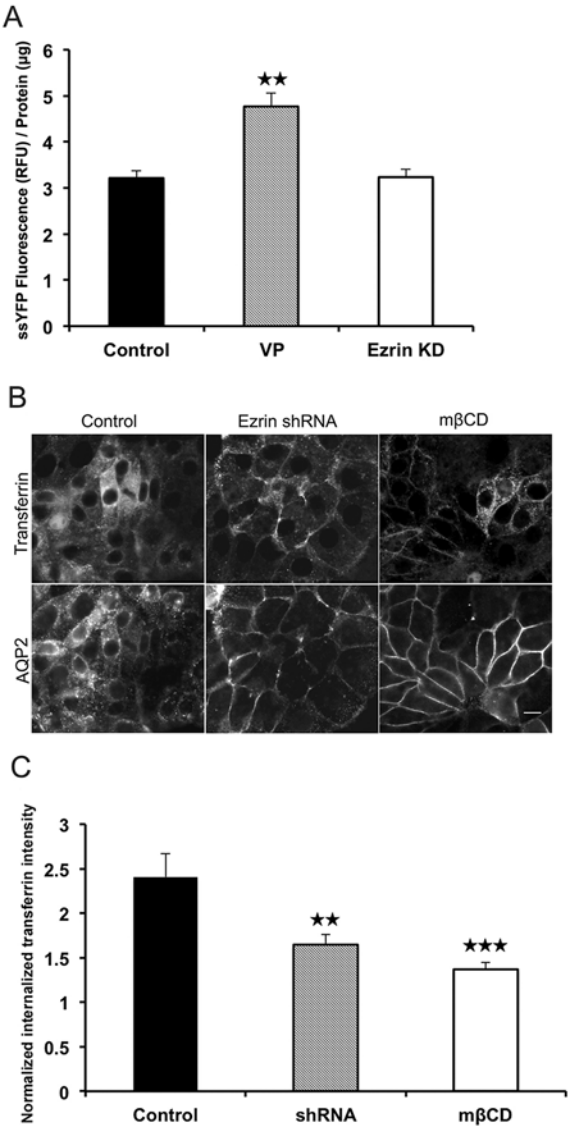

Fig. 7. Downregulating ezrin reduces clathrin-mediated endocytosis and causes concomitant membrane accumulation of AQP2 without affecting the overall exocytosis. (A) Ezrin knockdown does not affect the overall exocytosis in LLC-AQP2-ssYFP cells. LLC-AQP2 cells were stably transfected with ssYFP. The fluorescence signal in the extracellular medium was measured in LLC-AQP2-ssYFP cells with and without treatment with VP or ezrin shRNA lentivirus, respectively. The fluorescence intensity in the medium reflected the exocytotic activity of LLC-AQP2-ssYFP cells, and therefore the rate of exocytosis. No significant increase was seen in the overall exocytosis in LLC-AQP2-ssYFP cells treated with ezrin shRNA lentivirus compared to control. In contrast, a significant increase in exocytosis was observed in VP-treated LLC-AQP2-ssYFP cells, which is consistent with our previous reports (Nunes et al., 2008). (B) Endocytosis assay using Rhodamine-conjugated transferrin showed that Alexa Fluor 568-labeled transferrin accumulated on the apical membrane following ezrin knockdown (upper panel), and a simultaneous acute membrane accumulation of AQP2 (lower panel). Scale bar: 10 µm. (C) A bar graph showing that ezrin knockdown affects clathrin-mediated endocytosis. A block of endocytosis with MβCD was used as a positive control. Results in A and C are mean±s.e.m. ($n \geq 3$). $^{**}P<0.01$, $^{***}P<0.001$ (one-way ANOVA).

60 min into the cold block procedure. AQP2 internalization did ultimately occur in the presence of ezrin knockdown, but only after a significant delay (Fig. 8A). In addition, the accumulation of the AQP2 perinuclear patch progressed at a much slower rate compared to that in the control (Fig. 8B). This cold block experiment suggests that downregulation of ezrin specifically attenuates AQP2 endocytosis/internalization in cells.

DISCUSSION

AQP2 is a well-studied water channel that undergoes both regulated trafficking mediated by VP and constitutive recycling. After translocation from intracellular vesicles to the apical membrane of the collecting duct principal cell, AQP2 mediates water transport. Membrane accumulation of AQP2 is determined by exocytotic and endocytotic processes (Brown and Fenton, 2015). It is increasingly recognized that the dynamic regulation of the actin cytoskeleton network is critical for vesicle trafficking, exocytosis and endocytosis, and therefore for the proper targeting of AQP2 to the apical membrane (Noda et al., 2008; Tamma et al., 2001). However, the specific regulatory mechanisms are largely unknown. Here, we show that ezrin, a plasma membrane and actin cytoskeleton linker, is an AQP2-interacting protein. By performing pulldown and co-IP assays, we demonstrate that a direct interaction of ezrin and AQP2 occurs between the ezrin N-terminal FERM domain and the AQP2 C-terminus. Through this interaction with AQP2, ezrin facilitates the endocytosis of AQP2, which is independent of AQP2 phosphorylation and intracellular cAMP elevation.

ERM proteins function in the critical interface between the plasma membrane and underlying cell cortex. In addition to organizing and maintaining the cell cortex through interactions with the plasma membrane and filamentous actin, ERM proteins regulate multiple signaling pathways through their ability to bind transmembrane receptors and link them to downstream signaling components. Extensive *in vitro* and *in vivo* studies have demonstrated a multitude of critical cellular functions mediated by ERM proteins, ranging from cell membrane organization, formation of microvilli, regulation of cell extension and polarity, and cell adhesion and migration contributing to the immune response, vascular permeability and tumor progression (Amsellem et al., 2014). Most of these cellular functions involve a direct or indirect interaction of ERM proteins with transmembrane receptors, such as the hyaluronic acid receptor CD44, ICAM-2, ICAM-3, syndecan 2 and the α1β-adrenergic receptor, via its highly conserved N-terminal FERM domain (Donowitz et al., 2005; Granés et al., 2000; Helander et al., 1996; Reczek et al., 1997; Reczek and Bretscher, 1998; Scholl et al., 1999; Serrador et al., 1997; Stanasila et al., 2006). The ERM family member moesin has been implicated previously in AQP2 apical membrane targeting in cultured cells, but the specific mechanism was not defined (Tamma et al., 2005). A physical interaction between ERM proteins and AQP2 has never been reported. Our data reveal that the ERM protein ezrin directly interacts with AQP2 via its FERM domain.

It has been commonly accepted that ERM proteins exist in two interchangeable states, the dormant inactive state and the 'active' state. The 'inactive' state is a closed conformation in which the N-terminal FERM domain and the C-terminal actin-binding site are masked due to a strong self-interaction between the N-terminal domain and the C-terminal domain (Gary and Bretscher, 1995). They become active after the intramolecular interaction is relieved by the sequential binding of the FERM domain to phosphatidylinositol 4,5-biphosphate (PIP2) and subsequent phosphorylation of the conserved T567/T564/T568 residue in the C-terminal F-actin-binding domain of ERM proteins (Fievet et al., 2004). The active state can therefore interact with its binding partners through the exposed FERM domain. The major pool of ERM proteins in the cell is present in the cytoplasm, where it is thought to be in an inactive

Journal of Cell Science (2017) 130, 2914-2925 doi:10.1242/jcs.204842

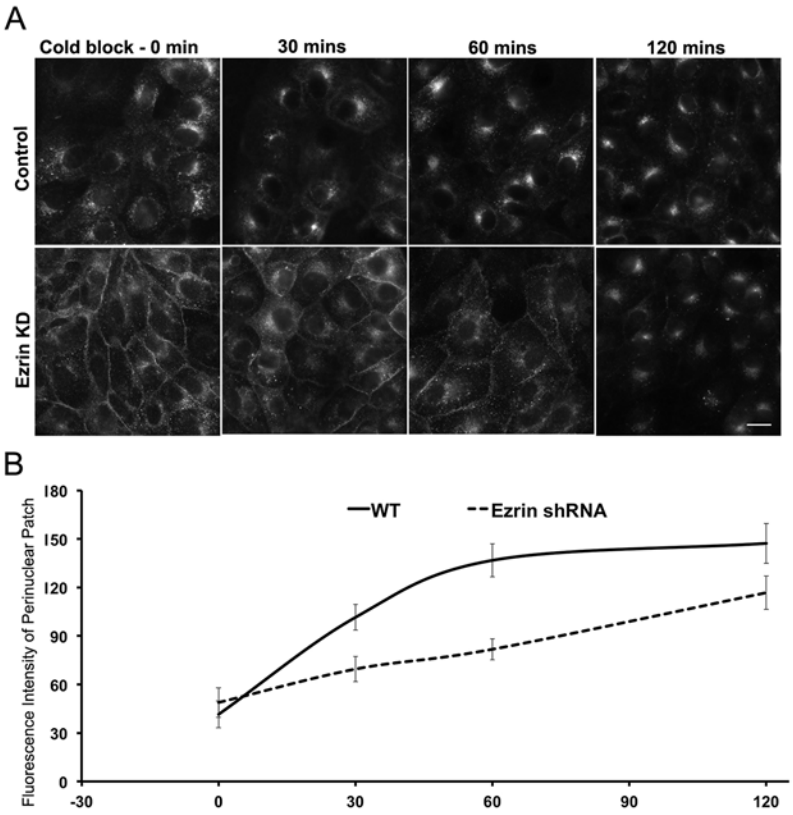

Fig. 8. AQP2 internalization was reduced after ezrin knockdown in a cold block experiment. (A) Dynamic distribution of AQP2 after a 20°C cold block was revealed by immunofluorescence staining of LLC-AQP2 cells. Cells were incubated at 20°C for 30, 60 and 120 min to block AQP2 release from the trans-Golgi network. AQP2 formed a 'perinuclear patch' in cells at 20°C. In the absence of protein synthesis (blocked by cycloheximide), the speed of formation and immunostaining intensity of the perinuclear patch reflect the speed and extent of AQP2 internalization from the cell surface over time. Scale bar: 10 µm. (B) Quantification of the growth of the AQP2-positive perinuclear patch after 20°C cold block over time. The fluorescence intensity of AQP2 staining in the perinuclear patch was measured using Volocity software as described previously (Arthur et al., 2015). Results are mean±s.e.m. ($n \geq 13$ for each data point). Experiments were repeated at least three times.

conformation. Interestingly, in our co-IP and pulldown experiments, we were able to detect the interaction of AQP2 with both full-length ezrin and the FERM-containing N-terminal ezrin protein. No interaction of AQP2 was detected with the recombinant protein that contains only the ezrin C-terminus. Despite the common belief that the active conformation of ezrin is required for interaction with membrane proteins, inactive ezrin is detected in plasma membrane isolates (Smith et al., 2003). In accordance with our data, the 'inactive' full-length ezrin has been shown to interact with PIP2 *in vitro* as well as the N-terminal FERM domain (Niggli et al., 1995). Dbl (also known as MCF2), a Rho-specific guanine nucleotide exchange factor, was shown to effectively bind both the N-terminal active mutant of ezrin and the full-length inactive molecule *in vitro* and *in vivo*, and Dbl induces localization of both the active and the full-length ezrin proteins to the plasma membrane, a process that does not require ezrin C-terminus phosphorylation (Vanni et al., 2004). Similarly, our data suggest that the interaction between ezrin and AQP2 does not require ezrin activation or phosphorylation.

Remarkably, VP treatment causes translocation of not only AQP2 but also ezrin to the plasma membrane from its initial cytosolic and basolateral location in both polarized MDCK cells and kidney collecting duct principal cells. It is conceivable that through interaction with AQP2, ezrin is recruited to the plasma membrane together with AQP2 in response to VP stimulation despite being in an inactive state. It is also possible that VP may phosphorylate ezrin and then phosphorylated ezrin translocates to the plasma membrane. Indeed, multiple proteins including PKA, protein kinase C and RhoA GTPase have been implicated in ERM phosphorylation and activation (Barile et al., 2005; Menager et al., 1999; Ng et al., 2001; Tran Quang et al., 2000; Zhou et al., 2003). Our data suggest that the effect of ezrin on AQP2 internalization does not depend on the AQP2 phosphorylation state, VP stimulation or elevation of intracellular cAMP. We cannot determine from our data whether VP phosphorylates ezrin through PKA or other signaling pathways. Nor do we yet understand the effect of concomitant phosphorylation of AQP2 and ezrin on their interaction and trafficking. These highly complex and interesting questions remain to be elucidated in future studies.

Nonetheless, our data show that knocking down ezrin leads to significant membrane accumulation of AQP2 due to a reduction of AQP2 endocytosis without any detectable impact on overall exocytosis. In recent years, an important role of ERM proteins in mediating vesicle and membrane protein trafficking including endocytosis, exocytosis and recycling is emerging (Barroso-González et al., 2009; Cha et al., 2006; Stanasila et al., 2006; Zhao et al., 2004; Zhou et al., 2005). Ezrin regulates recycling/exocytosis of the α1β-adrenergic receptor, and membrane insertion of H^+-K^+-ATPase in parietal cells (Yu et al., 2014; Zhou et al., 2005). Ezrin and Sec3 form complexes mediating mucin (MUC5AC) secretion in neutrophil elastase-stimulated airway epithelial cells (Qin et al., 2015). Ezrin also facilitates the exocytosis and plasma membrane delivery of newly synthesized epithelial brush-border (BB) Na^+/H^+ antiporter 3 (NHE3), and tethers the γ-aminobutyric acid transporter GAT1 to actin filaments during postsynaptic uptake of GAT1 (Cha et al., 2006; Imoukhuede et al., 2009; Zhao et al., 2004). Despite these observations, the precise roles of the ERM protein ezrin in endocytosis versus exocytosis, and recycling of membrane proteins are not understood mechanistically. Our data suggest that ezrin is important for AQP2 internalization, probably via its interaction with actin.

In summary, we have identified ezrin as an AQP2-interacting protein. Through direct interaction with AQP2, ezrin facilitates the endocytosis of AQP2 independently of VP action, AQP2 phosphorylation or cAMP elevation. Identification of this direct

Journal of Cell Science (2017) 130, 2914-2925 doi:10.1242/jcs.204842

interaction between AQP2 and ezrin contributes to the understanding of AQP2 trafficking and its regulatory mechanisms.

MATERIALS AND METHODS

Reagents, chemicals, constructs and cell culture

Unless otherwise specified, all chemicals were purchased from Sigma-Aldrich (St Louis, MO). Alexa Fluor 568-conjugated transferrin was purchased from Molecular Probes (Invitrogen/Thermo Fisher Scientific, Waltham, MA). Sulfo-NHS-LC-Biotin was purchased from Thermo Fisher Scientific and streptavidin-coupled Dynabeads from Invitrogen. Histidine (His)-tag Dynabeads and protein A Dynabeads were also purchased from Invitrogen, and Glutathione Sepharose 4 Fast Flow and HisPrep FF 16/10 for protein purification from GE Healthcare (Marlborough, MA).

Monoclonal antibodies against c-Myc were generated in-house from the 9E10 hybridoma cell line obtained from the American Type Culture Collection (ATCC, Manassas, VA). Secondary antibodies tagged with either indocarbocyanine (Cy3) or fluorescein isothiocyanate (FITC) were obtained from Jackson Immunoresearch Laboratories (West Grove, PA). The antibody against total AQP2, and various phosphorylation-specific AQP2 antibodies, that were used for co-IP and mass spectrometry experiments, were generated and kindly given by Dr Mark Knepper (NIH, Bethesda, MD). The commercial primary antibodies are from the following vendors: rabbit polyclonal anti-AQP2 antibody (#AQP2-002, Alomone Labs, Jerusalem, Israel), goat polyclonal anti-AQP2 antibody (sc9882, Santa Cruz Biotechnology, Dallas, TX), rabbit polyclonal anti-ezrin (3145s, Cell Signaling), rabbit anti-AQP2 p256 (PhosphoSolutions, Aurora, CO, USA), rabbit anti-AQP2 p261 (PhosphoSolutions), mouse monoclonal anti-GST antibody (sc138, Santa Cruz Biotechnology), mouse monoclonal anti-His antibody (70796, EMD Millipore, Billerica, MA), mouse anti-GAPDH antibody (AM4300, Ambion/Thermo Fisher Scientific), mouse anti β-actin antibody (A5441, Sigma-Aldrich), and rabbit anti-transferrin receptor 1 antibody (ab84036, Abcam, Cambridge, MA). Commercial secondary horseradish peroxidase (HRP)-conjugated donkey anti-goat-IgG, donkey anti-rabbit-IgG, and donkey anti-mouse-IgG antibodies from Santa Cruz Biotechnology were used according to the manufacturer's protocol. Table S1 shows the dilutions at which primary antibodies were used.

Ezrin constructs for a His_6-tagged fusion protein of full-length human ezrin, the N-terminal domain of ezrin (amino acids 1–308) and a C-terminal portion of ezrin (amino acids 285–586) were cloned in a pET30a vector. MDCK and LLC-PK1 cells stably expressing rat AQP2 were generated as described previously (Lu et al., 2004; Rice et al., 2012; Yui et al., 2009). All cell lines were maintained in Dulbecco's modified Eagle's medium (DMEM) supplemented with 10% bovine serum and 1% penicillin/streptomycin at 37°C in a 5% CO_2 atmosphere incubator.

Ezrin knock-down in cells

The ezrin short hairpin RNA (shRNA) plasmids were gifts from Dr Tomas Kirchhausen (Children's Hospital and Harvard Medical School, Boston, MA). The following targeting sequences were used: no. 1, 5′-CCTGGAA-ATGTATGGAATCAA-3′; no. 2, 5′-CCAGCCAAATACAACTGGAAA-3′; no. 3, 5′-CCCACGTCTGAGAATCAACAA-3′; no. 4, 5′-CGTGGGA-TGCTCAAAGATAAT-3′; and no. 5, 5′-CTCCACTATGTGGATAATAA-A-3′. The five different shRNA lentivirus (pLKO.1) products were combined and used to infect stable AQP2-expressing LLC-PK1 cells (LLC-AQP2) with 5 µg/ml polybrene (EMD Millipore). The shRNA plasmid was co-transfected with packaging vector pRSV-REV (Addgene, Cambridge, MA) and envelope vector pCMV-VSV-G (Addgene) into HEK293T cells. The supernatant containing lentivirus was collected after 60 h post transfection and centrifuged at 5000 ***g***, 4°C for 10 min to remove cell debris. The virus-containing supernatant was aliquoted and stored at −80°C until use.

Animals

Animal experiments were approved by the Massachusetts General Hospital (MGH) Institutional Committee on Research Animal Care, in accordance with National Institutes of Health (NIH) Guide for the Care and Use of Laboratory Animals. The VP analog DDAVP (Sigma-Aldrich) was delivered to adult male Brattleboro rats (Rat Resource and Research Center, Columbia, MO) at 1.2 µg/day for 7 days via a subcutaneous Alzet osmotic pump (Durect, Cupertino, CA) that was implanted under the neck skin as previously described (Bagnis et al., 2001; Paunescu et al., 2013). Control and DDAVP-treated Brattleboro rats were anesthetized by isoflurane inhalation and were euthanized by exsanguination. The kidneys were collected and were cut into thin slices and fixed with modified PLP fixative (4% paraformaldehyde, 75 mM lysine, 10 mM sodium periodate and 5% sucrose in 37.5 mM sodium phosphate buffer) by immersion. After washing with PBS, kidney tissues were embedded in Tissue-Tek OCT compound 4583 (Sakura Finetek USA, Torrance, CA) and processed for cryosectioning and immunofluorescence staining as previously described (Rice et al., 2015; Vedovelli et al., 2013).

Immunofluorescence staining and immunoblotting

8×10^3 stable AQP2-expressing MDCK (MDCK-AQP2) cells were plated on Transwell filters (Costar 3460, Corning, Corning, NY) in 12-well plates. Polarized monolayers were formed after 3 days for MDCK cells. LLC-PK1 cells were plated on multiple 10×10 mm glass coverslips (Electron Microscopy Sciences, Hatfield, PA) and allowed to grow to 90% confluence. Arginine vasopressin (AVP, 20 nM) was added to MDCK-AQP2 cells; lysine-vasopressin (LVP) (20 nM) was added to LLC-PK1 cells because they are derived from porcine kidney. After incubation for 20 min, cells were fixed with 4% paraformaldehyde (PFA) in phosphate-buffered saline (PBS) (pH 7.4) for 20 min and subjected to a previously described immunostaining protocol (Rice et al., 2012). After permeabilization with 0.01% Triton X-100 in PBS for 4 min and a 30 min block with 1% bovine serum albumin (BSA) in PBS, cells were incubated with the primary antibody overnight at 4°C. The next day, cells were washed three times with PBS, and then incubated with the fluorescent tag-conjugated secondary antibodies for 1 h at room temperature. For immunofluorescence staining of kidney tissue, the kidney slices were treated with 0.01% SDS in PBS for permeabilization (Brown et al., 1996) and then subjected to a similar immunostaining protocol but without the Triton X-100 step. Subsequently, the coverslips and kidney sections were washed and mounted in Vectashield containing DAPI nuclear stain (Vector Labs, Burlingame, CA) and visualized on a Nikon 80i microscope with an ORCA95 camera (Hamamatsu, Tokyo, Japan). Images were captured using IPLab software (BD Biosciences, San Jose, CA). Confocal imaging was performed using a Zeiss LSM800 confocal microscope with an Airyscan module (Carl Zeiss, Jena, Germany). Image brightness and contrast were linearly adjusted, and a high-pass filter was applied to remove noise and sharpen images in Photoshop software (Adobe Systems Inc., San Jose, CA, USA).

For immunoblotting, cell lysates were separated by SDS-PAGE under reducing conditions. Proteins were transferred to polyvinylidene fluoride (PVDF) membranes by electroblotting using a semi-dry apparatus (Bio-Rad). Ezrin or AQP2 were detected on the blots with the appropriate polyclonal antibodies, followed by anti-goat-IgG or anti-rabbit-IgG coupled to HRP. Detection was achieved using a chemiluminescent probe (ECL; Amersham/GE Healthcare, Marlborough, MA, USA).

Expression and purification of recombinant proteins

Escherichia coli, BL21 (DE3) (Novagen/EMD Millipore) was used for His- and GST-tag fusion protein expression. GST–AQP2 C-terminal fusion proteins were generated as described previously (Lu et al., 2007). Expression of His–ezrin in *E. coli* was induced by 1 mM isopropyl 1-thio-β-D-galactopyranoside (IPTG) at 37°C for 4 h. Bacteria were lysed with lysozyme (1 mg/ml) and 0.1% Triton X-100 in sodium chloride-Tris-EDTA (STE) buffer (150 mM NaCl, 50 mM Tris-HCl, 1 mM EDTA, pH 7.4) and sonicated for 15 min at 20% energy in an ice bath using a Misonix Sonicator XL (Farmingdale, NY). After centrifugation to remove bacterial debris, the supernatant was allowed to bind to the Ni column at 4°C for 40 min with gentle rocking. After washing twice with STE buffer containing 500 mM NaCl and 0.1% Triton X-100 and three times with regular STE buffer, fusion protein was eluted with elution buffer (200 mM imidazole in STE buffer) and dialyzed against PBS at 4°C overnight. Purified fusion proteins were subsequently subjected to SDS-PAGE and immunoblot analysis, and used for pulldown experiments.

Cell surface biotinylation

Cell surface biotinylation was performed as previously described (Lu et al., 2004). Briefly, after VP treatment, stable AQP2-expressing LLC-PK1 cells

Journal of Cell Science

(LLC-AQP2 cells) were incubated with sulfo-NHS-LC-Biotin (0.5 mg/ml) at 4°C for 1 h. 1 M Tris-HCl at pH 7.4 was added to quench the reaction. After being washed three times with cold PBS, cells were scraped into cold lysis buffer [PBS containing 0.5% Nonidet P-40 (NP-40), 0.1% Triton X-100, protease inhibitor cocktail and phosphatase inhibitor cocktail] and incubated at 4°C for 30 min. Pulldown experiments were performed using streptavidin-coupled Dynabeads (Invitrogen) following the manufacturer's instructions. Briefly, surface biotinylated cell lysates were incubated with Dynabeads at 4°C for 3 h followed by washing with gentle rocking, then subjected to three PBS washes followed by SDS-PAGE and immunoblotting. Anti-AQP2 and anti-ezrin antibodies were used to detect the respective proteins in the surface biotinylated membrane protein pool. Anti-transferrin receptor 1 antibody was used to detect the surface-labeled resident membrane receptor to be used as input reference.

Co-IP and pulldown assays

Co-IP was performed as previously described (Lu et al., 2007). Briefly, transfected or non-transfected LLC-AQP2 cells from one 100-mm^2 culture plate were harvested. After three washes with cold PBS, cells were scraped into cold lysis buffer containing 8 mM NaF, 4 mM Na_3VO_4, 0.1% Triton X-100, 0.5% NP-40 and protease inhibitor cocktail in PBS. Cell lysates were passed five times through a 27-gauge syringe and centrifuged at 8000 ***g*** for 10 min at 4°C and supernatants were collected. Kidney papilla extract was prepared from mouse kidney. The kidney papillae were washed three times with cold PBS and homogenized in a Teflon pestle homogenizer (Thomas Scientific, Swedesboro, NJ). After passing through a syringe with a 27-gauge needle at least five times, the homogenates were resuspended in cold lysis buffer as described above plus 0.1% SDS and centrifuged at 8000 ***g*** for 10 min at 4°C to collect supernatants. These cell lysates and kidney papilla extracts were used for pulldown and co-IP experiments. To ensure the completeness of the kidney tissue membrane solubilization, we frequently passed the lysates through a 27-gauge syringe more than five times, and added SDS (0.1%) to the kidney homogenates to further increase the solubility of the membrane component.

LLC-AQP2 cell lysates and kidney papilla extracts were pre-cleared using protein A beads. Approximately 500 µl lysate were incubated with protein A beads (40 µl) and 0.5 µg antibody at 4°C for 3 h. After washing five times (PBS with 0.1% Tween 20), the co-IP samples were subjected to SDS-PAGE and immunoblotting. Cell lysates incubated with protein A beads alone were routinely used as a negative control. Lysates of non-transfected cells were also used as negative control in each co-IP experiment. All experiments were repeated at least three times.

Pulldown assays were performed as previously described (Lu et al., 2007). LLC-AQP2 lysates and papilla extracts were pre-cleared on a glutathione column at 4°C for 40 min with rocking. Approximately 4 µg of the His–ezrin proteins were incubated with 40 µl His-tag Dynabeads and 0.5–1 mg pre-cleared cell lysate or mouse kidney papilla extract at 4°C with gentle rocking for 2 h. To remove nonspecifically bound proteins, the Dynabead complex was washed four times with PBS containing 0.1% Tween 20. Finally, the pulled down complex was subjected to SDS-PAGE and immunoblotting.

cAMP assay

LLC-AQP2 cells were plated onto 96-well plates and grown to confluence. The intracellular cAMP assay was performed using the Direct cAMP ELISA kit (Enzo Life Sciences, Farmingdale, NY, USA). Briefly, cells were transfected with ezrin shRNA for 48 h or treated with VP (20 nM) for 30 min. The cells were then lysed and centrifuged, and the supernatant was added to 96-well plates precoated with donkey anti-rabbit-IgG antibody, and then mixed with rabbit anti-cAMP antibody. After washing, cAMP-conjugated alkaline phosphatase was added for 2 h. After washing the plate, the substrate p-nitrophenyl phosphate was added. After incubation for 60 min at room temperature, trisodium phosphate was added to terminate the reaction. The optical density (OD) was read on a plate reader at 405 nm. ODs were compared with standards to determine the level of cAMP (0–20 pmol/ml). The intracellular cAMP assay was performed in triplicate.

Endocytosis and exocytosis assays

The endocytosis assay was performed in LLC-AQP2 cells as described previously (Lu et al., 2004). Briefly, cells were seeded in a 24-well cell culture plate, and transfected with ezrin shRNA for 48 h. Transfected cells were then incubated with 25 µg/ml transferrin conjugated with Alexa Fluor 568 at 37°C for 30 min with gentle rocking. After three washes with cold PBS, cells were fixed with 4% PFA in PBS and subjected to the immunofluorescence staining protocol described above.

The exocytosis assay was performed as previously described in LLC-AQP2 cells that stably express soluble secreted yellow fluorescent protein LLC-AQP2-ssYFP (Nunes et al., 2008). Briefly, LLC-AQP2 cells stably expressing soluble secreted yellow fluorescent protein (ssYFP) were established and named LLC-AQP2-ssYFP. The LLC-AQP2-ssYFP cells were seeded in 12-well plates and transfected with ezrin shRNA lentivirus. After washing with PBS twice, cells were incubated with Hank's balanced salt solution (HBSS, 1×) for 1 h at 37°C before performing the assay. LVP was added to some wells to stimulate exocytosis and served as the positive control. At the end of the 1 h incubation, 150 µl of medium were transferred from each well to individual wells of a 96-well plate for detecting the fluorescence signal using a multimode plate reader (model DTX880, Beckman-Coulter, Fullerton, CA).

Cold block assay

The 20°C cold block assay was performed as previously described (Rice et al., 2012). When cells are incubated at this temperature, newly synthesized and recycling proteins are prevented from exiting the TGN compartment and entering the exocytotic pathway, which results in their perinuclear accumulation (Griffiths et al., 1985). LLC-AQP2 cells were plated on 10×10 mm glass coverslips (Electron Microscopy Sciences, Hatfield, PA) and allowed to grow to 90% confluence. Cycloheximide (10 µg/ml) was added to cells 60 min before the cold block to inhibit protein synthesis, so that only recycling proteins accumulate in the TGN after being internalized from the cell surface. Cells were incubated in a 20°C water bath placed in a cold room for up to 120 min. Coverslips were harvested at different time points and fixed with 4% PFA in PBS and subjected to immunofluorescence staining as detailed above.

For image quantification, all coverslips were immunostained under the same conditions and imaged with the same microscope/camera parameters. Analysis of the fluorescence intensity of the perinuclear patch resulting from the cold block was performed using ImageJ software (National Institutes of Health, Bethesda, MD). The region of interest used to measure AQP2 patch fluorescence was determined by applying an intensity threshold to the visible perinuclear accumulation of AQP2.

Statistical analysis

Statistics were performed with the Prism software (GraphPad Software Inc., La Jolla, CA, USA). All groups were first compared for significance with a one-way ANOVA. A two-tailed *t*-test was applied to determine the difference between individual groups, and $P<0.05$ was considered significant. Data were obtained from at least three independent experiments for each experimental condition.

Acknowledgements

The authors would like to thank Dr Quanhong Qi for her technical assistance and Dr Matthew J. Mahon for helpful discussions of the project. The authors also thank Dr Tomas Kirchhausen for the kind gift of ezrin shRNA plasmids. The Zeiss LSM800 Airyscan system was purchased using an NIH Shared Instrumentation Grant (S10 OD021577-01) to D.B. S.C. is supported by Telethon Foundation, Italy (GGP13227). Additional support for the Program in Membrane Biology Microscopy Core comes from the Boston Area Diabetes and Endocrinology Research Center (DK57521) and the MGH Center for the Study of Inflammatory Bowel Disease (DK43351).

Competing interests

The authors declare no competing or financial interests.

Author contributions

Conceptualization: H.A.J.L.; Methodology: W.L., K.T., Y.C., H.A.J.L.; Validation: W.L., K.T., H.A.J.L.; Formal analysis: W.L., H.A.J.L.; Investigation: W.L., W.W.J., K.T., Y.C., N.N., L.S., N.Y., J.A., H.A.J.L.; Resources: W.L., W.W.J., K.T., Y.C., N.N., L.S., N.Y., J.A., S.C., T.G.P., D.B., H.A.J.L.; Data curation: W.L., K.T., H.A.J.L.; Writing - original draft: W.L., H.A.J.L.; Writing - review & editing: W.L., W.W.J., K.T., Y.C., N.N., L.S., N.Y., J.A., S.C., T.G.P., D.B., H.A.J.L.; Visualization: W.L., K.T., T.G.P., H.A.J.L.; Supervision: H.A.J.L.; Project administration: H.A.J.L.; Funding acquisition: H.A.J.L.

Funding
HAJL is supported by the National Institutes of Health (NIH) (R01DK096015 and R21DK092619), the NephCure Foundation, a Gottschalk research grant from the American Society of Nephrology, and the Massachusetts General Hospital Executive Committee on Research. D.B. is supported by the NIH (R01DK096586). Deposited in PMC for release after 12 months.

Supplementary information
Supplementary information available online at
http://jcs.biologists.org/lookup/doi/10.1242/jcs.204842.supplemental

References

Amsellem, V., Dryden, N. H., Martinelli, R., Gavins, F., Almagro, L., Birdsey, G. M., Haskard, D. O., Mason, J. C., Turowski, P. and Randi, A. M. (2014). ICAM-2 regulates vascular permeability and N-cadherin localization through ezrin-radixin-moesin (ERM) proteins and Rac-1 signalling. *Cell Commun. Signal.* **12**, 12.

Arthur, J., Huang, J., Nomura, N., Jin, W. W., Li, W., Cheng, X., Brown, D. and Lu, H. J. (2015). Characterization of the putative phosphorylation sites of the AQP2 C terminus and their role in AQP2 trafficking in LLC-PK$_1$ cells. *Am. J. Physiol. Renal. Physiol.* **309**, F673-F679.

Bagnis, C., Marshansky, V., Breton, S. and Brown, D. (2001). Remodeling the cellular profile of collecting ducts by chronic carbonic anhydrase inhibition. *Am. J. Physiol. Renal. Physiol.* **280**, F437-F448.

Barile, M., Pisitkun, T., Yu, M.-J., Chou, C.-L., Verbalis, M. J., Shen, R.-F. and Knepper, M. A. (2005). Large scale protein identification in intracellular aquaporin-2 vesicles from renal inner medullary collecting duct. *Mol. Cell. Proteomics* **4**, 1095-1106.

Barroso-González, J., Machado, J.-D., Garcia-Expósito, L. and Valenzuela-Fernández, A. (2009). Moesin regulates the trafficking of nascent clathrin-coated vesicles. *J. Biol. Chem.* **284**, 2419-2434.

Berryman, M., Franck, Z. and Bretscher, A. (1993). Ezrin is concentrated in the apical microvilli of a wide variety of epithelial cells whereas moesin is found primarily in endothelial cells. *J. Cell Sci.* **105**, 1025-1043.

Bretscher, A. (1983). Purification of an 80,000-dalton protein that is a component of the isolated microvillus cytoskeleton, and its localization in nonmuscle cells. *J. Cell Biol.* **97**, 425-432.

Brown, D. and Fenton, R. (2015). *The Cell Biology of Vasopressin Action*. Philadelphia, USA: Elsevier Inc.

Brown, D., Lydon, J., McLaughlin, M., Stuart-Tilley, A., Tyszkowski, R. and Alper, S. (1996). Antigen retrieval in cryostat tissue sections and cultured cells by treatment with sodium dodecyl sulfate (SDS). *Histochem. Cell Biol.* **105**, 261-267.

Cha, B., Tse, M., Yun, C., Kovbasnjuk, O., Mohan, S., Hubbard, A., Arpin, M. and Donowitz, M. (2006). The NHE3 juxtamembrane cytoplasmic domain directly binds ezrin: dual role in NHE3 trafficking and mobility in the brush border. *Mol. Biol. Cell* **17**, 2661-2673.

Donowitz, M., Cha, B., Zachos, N. C., Brett, C. L., Sharma, A., Tse, C. M. and Li, X. (2005). NHERF family and NHE3 regulation. *J. Physiol.* **567**, 3-11.

Fievet, B. T., Gautreau, A., Roy, C., Del Maestro, L., Mangeat, P., Louvard, D. and Arpin, M. (2004). Phosphoinositide binding and phosphorylation act sequentially in the activation mechanism of ezrin. *J. Cell Biol.* **164**, 653-659.

Gary, R. and Bretscher, A. (1995). Ezrin self-association involves binding of an N-terminal domain to a normally masked C-terminal domain that includes the F-actin binding site. *Mol. Biol. Cell* **6**, 1061-1075.

Granés, F., Urena, J. M., Rocamora, N. and Vilaró, S. (2000). Ezrin links syndecan-2 to the cytoskeleton. *J. Cell Sci.* **113**, 1267-1276.

Griffiths, G., Pfeiffer, S., Simons, K. and Matlin, K. (1985). Exit of newly synthesized membrane proteins from the trans cisterna of the Golgi complex to the plasma membrane. *J. Cell Biol.* **101**, 949-964.

Hays, R. M., Condeelis, J., Gao, Y., Simon, H., Ding, G. and Franki, N. (1993). The effect of vasopressin on the cytoskeleton of the epithelial cell. *Pediatr. Nephrol.* **7**, 672-679.

Helander, T. S., Carpén, O., Turunen, O., Kovanen, P. E., Vaheri, A. and Timonen, T. (1996). ICAM-2 redistributed by ezrin as a target for killer cells. *Nature* **382**, 265-268.

Hunter, T. and Cooper, J. A. (1981). Epidermal growth factor induces rapid tyrosine phosphorylation of proteins in A431 human tumor cells. *Cell* **24**, 741-752.

Imoukhuede, P. I., Moss, F. J., Michael, D. J., Chow, R. H. and Lester, H. A. (2009). Ezrin mediates tethering of the gamma-aminobutyric acid transporter GAT1 to actin filaments via a C-terminal PDZ-interacting domain. *Biophys. J.* **96**, 2949-2960.

Klussmann, E., Tamma, G., Lorenz, D., Wiesner, B., Maric, K., Hofmann, F., Aktories, K., Valenti, G. and Rosenthal, W. (2001). An inhibitory role of Rho in the vasopressin-mediated translocation of aquaporin-2 into cell membranes of renal principal cells. *J. Biol. Chem.* **276**, 20451-20457.

Li, W., Zhang, Y., Bouley, R., Chen, Y., Matsuzaki, T., Nunes, P., Hasler, U., Brown, D. and Lu, H. A. J. (2011). Simvastatin enhances aquaporin-2 surface expression and urinary concentration in vasopressin-deficient Brattleboro rats through modulation of Rho GTPase. *Am. J. Physiol. Renal. Physiol.* **301**, F309-F318.

Lu, H., Sun, T. X., Bouley, R., Blackburn, K., McLaughlin, M. and Brown, D. (2004). Inhibition of endocytosis causes phosphorylation (S256)-independent plasma membrane accumulation of AQP2. *Am. J. Physiol. Renal. Physiol.* **286**, F233-F243.

Lu, H. A. J., Sun, T.-X., Matsuzaki, T., Yi, X.-H., Eswara, J., Bouley, R., McKee, M. and Brown, D. (2007). Heat shock protein 70 interacts with aquaporin-2 and regulates its trafficking. *J. Biol. Chem.* **282**, 28721-28732.

McClatchey, A. I. and Fehon, R. G. (2009). Merlin and the ERM proteins – regulators of receptor distribution and signaling at the cell cortex. *Trends Cell Biol.* **19**, 198-206.

Menager, C., Vassy, J., Doliger, C., Legrand, Y. and Karniguian, A. (1999). Subcellular localization of RhoA and ezrin at membrane ruffles of human endothelial cells: differential role of collagen and fibronectin. *Exp. Cell Res.* **249**, 221-230.

Ng, T., Parsons, M., Hughes, W. E., Monypenny, J., Zicha, D., Gautreau, A., Arpin, M., Gschmeissner, S., Verveer, P. J., Bastiaens, P. I. et al. (2001). Ezrin is a downstream effector of trafficking PKC-integrin complexes involved in the control of cell motility. *EMBO J.* **20**, 2723-2741.

Nielsen, S., Terris, J., Andersen, D., Ecelbarger, C., Frokiaer, J., Jonassen, T., Marples, D., Knepper, M. A. and Petersen, J. S. (1997). Congestive heart failure in rats is associated with increased expression and targeting of aquaporin-2 water channel in collecting duct. *Proc. Natl. Acad. Sci. USA* **94**, 5450-5455.

Niggli, V., Andréoli, C., Roy, C. and Mangeat, P. (1995). Identification of a phosphatidylinositol-4,5-bisphosphate-binding domain in the N-terminal region of ezrin. *FEBS Lett.* **376**, 172-176.

Noda, Y., Horikawa, S., Kanda, E., Yamashita, M., Meng, H., Eto, K., Li, Y., Kuwahara, M., Hirai, K., Pack, C. et al. (2008). Reciprocal interaction with G-actin and tropomyosin is essential for aquaporin-2 trafficking. *J. Cell Biol.* **182**, 587-601.

Nunes, P., Hasler, U., McKee, M., Lu, H. A. J., Bouley, R. and Brown, D. (2008). A fluorimetry-based ssYFP secretion assay to monitor vasopressin-induced exocytosis in LLC-PK1 cells expressing aquaporin-2. *Am. J. Physiol. Cell Physiol.* **295**, C1476-C1487.

Parameswaran, N., Matsui, K. and Gupta, N. (2011). Conformational switching in ezrin regulates morphological and cytoskeletal changes required for B cell chemotaxis. *J. Immunol.* **186**, 4088-4097.

Paunescu, T. G., Lu, H. A. J., Russo, L. M., Pastor-Soler, N. M., McKee, M., McLaughlin, M. M., Bartlett, B. E., Breton, S. and Brown, D. (2013). Vasopressin induces apical expression of caveolin in rat kidney collecting duct principal cells. *Am. J. Physiol. Renal. Physiol.* **305**, F1783-F1795.

Procino, G., Barbieri, C., Carmosino, M., Tamma, G., Milano, S., De Benedictis, L., Mola, M. G., Lazo-Fernandez, Y., Valenti, G. and Svelto, M. (2011). Fluvastatin modulates renal water reabsorption in vivo through increased AQP2 availability at the apical plasma membrane of collecting duct cells. *Pflugers Arch.* **462**, 753-766.

Qin, L.-T., Wu, J., Mo, L.-Y., Zeng, H.-H. and Liang, Y.-P. (2015). Linear regression model for predicting interactive mixture toxicity of pesticide and ionic liquid. *Environ. Sci. Pollut. Res. Int.* **22**, 12759-12768.

Reczek, D. and Bretscher, A. (1998). The carboxyl-terminal region of EBP50 binds to a site in the amino-terminal domain of ezrin that is masked in the dormant molecule. *J. Biol. Chem.* **273**, 18452-18458.

Reczek, D., Berryman, M. and Bretscher, A. (1997). Identification of EBP50: a PDZ-containing phosphoprotein that associates with members of the ezrin-radixin-moesin family. *J. Cell Biol.* **139**, 169-179.

Rice, W. L., Zhang, Y., Chen, Y., Matsuzaki, T., Brown, D. and Lu, H. A. J. (2012). Differential, phosphorylation dependent trafficking of AQP2 in LLC-PK1 cells. *PLoS ONE* **7**, e32843.

Rice, W. L., Li, W., Mamuya, F., McKee, M., Paunescu, T. G. and Lu, H. A. (2015). Polarized Trafficking of AQP2 Revealed in Three Dimensional Epithelial Culture. *PLoS ONE* **10**, e0131719.

Rodal, S. K., Skretting, G., Garred, O., Vilhardt, F., van Deurs, B. and Sandvig, K. (1999). Extraction of cholesterol with methyl-beta-cyclodextrin perturbs formation of clathrin-coated endocytic vesicles. *Mol. Biol. Cell* **10**, 961-974.

Sabolić, I., Katsura, T., Verbavatz, J.-M. and Brown, D. (1995). The AQP2 water channel: effect of vasopressin treatment, microtubule disruption, and distribution in neonatal rats. *J. Membr. Biol.* **143**, 165-175.

Scholl, F. G., Gamallo, C., Vilaró, S. and Quintanilla, M. (1999). Identification of PA2.26 antigen as a novel cell-surface mucin-type glycoprotein that induces plasma membrane extensions and increased motility in keratinocytes. *J. Cell Sci.* **112**, 4601-4613.

Serrador, J. M., Alonso-Lebrero, J. L., del Pozo, M. A., Furthmayr, H., Schwartz-Albiez, R., Calvo, J., Lozano, F. and Sánchez-Madrid, F. (1997). Moesin interacts with the cytoplasmic region of intercellular adhesion molecule-3 and is redistributed to the uropod of T lymphocytes during cell polarization. *J. Cell Biol.* **138**, 1409-1423.

Smith, W. J., Nassar, N., Bretscher, A., Cerione, R. A. and Karplus, P. A. (2003). Structure of the active N-terminal domain of Ezrin. Conformational and mobility changes identify keystone interactions. *J. Biol. Chem.* **278**, 4949-4956.

Stanasila, L., Abuin, L., Diviani, D. and Cotecchia, S. (2006). Ezrin directly interacts with the alpha1b-adrenergic receptor and plays a role in receptor recycling. *J. Biol. Chem.* **281**, 4354-4363.

Subtil, A., Gaidarov, I., Kobylarz, K., Lampson, M. A., Keen, J. H. and McGraw, T. E. (1999). Acute cholesterol depletion inhibits clathrin-coated pit budding. *Proc. Natl. Acad. Sci. USA* **96**, 6775-6780.

Sun, T.-X., Van Hoek, A., Huang, Y., Bouley, R., McLaughlin, M. and Brown, D. (2002). Aquaporin-2 localization in clathrin-coated pits: inhibition of endocytosis by dominant-negative dynamin. *Am. J. Physiol. Renal. Physiol.* **282**, F998-F1011.

Tamma, G., Klussmann, E., Maric, K., Aktories, K., Svelto, M., Rosenthal, W. and Valenti, G. (2001). Rho inhibits cAMP-induced translocation of aquaporin-2 into the apical membrane of renal cells. *Am. J. Physiol. Renal. Physiol.* **281**, F1092-F1101.

Tamma, G., Klussmann, E., Procino, G., Svelto, M., Rosenthal, W. and Valenti, G. (2003). cAMP-induced AQP2 translocation is associated with RhoA inhibition through RhoA phosphorylation and interaction with RhoGDI. *J. Cell Sci.* **116**, 1519-1525.

Tamma, G., Klussmann, E., Oehlke, J., Krause, E., Rosenthal, W., Svelto, M. and Valenti, G. (2005). Actin remodeling requires ERM function to facilitate AQP2 apical targeting. *J. Cell Sci.* **118**, 3623-3630.

Tran Quang, C., Gautreau, A., Arpin, M. and Treisman, R. (2000). Ezrin function is required for ROCK-mediated fibroblast transformation by the Net and Dbl oncogenes. *EMBO J.* **19**, 4565-4576.

Tsukita, S., Oishi, K., Sato, N., Sagara, J., Kawai, A. and Tsukita, S. (1994). ERM family members as molecular linkers between the cell surface glycoprotein CD44 and actin-based cytoskeletons. *J. Cell Biol.* **126**, 391-401.

Turunen, O., Wahlstrom, T. and Vaheri, A. (1994). Ezrin has a COOH-terminal actin-binding site that is conserved in the ezrin protein family. *J. Cell Biol.* **126**, 1445-1453.

Vanni, C., Parodi, A., Mancini, P., Visco, V., Ottaviano, C., Torrisi, M. R. and Eva, A. (2004). Phosphorylation-independent membrane relocalization of ezrin following association with Dbl in vivo. *Oncogene* **23**, 4098-4106.

Vedovelli, L., Rothermel, J. T., Finberg, K. E., Wagner, C. A., Azroyan, A., Hill, E., Breton, S., Brown, D. and Paunescu, T. G. (2013). Altered V-ATPase expression in renal intercalated cells isolated from B1 subunit-deficient mice by fluorescence-activated cell sorting. *Am. J. Physiol. Renal. Physiol.* **304**, F522-F532.

Yonemura, S., Tsukita, S. and Tsukita, S. (1999). Direct involvement of ezrin/radixin/moesin (ERM)-binding membrane proteins in the organization of microvilli in collaboration with activated ERM proteins. *J. Cell Biol.* **145**, 1497-1509.

Yu, H., Zhou, J., Takahashi, H., Yao, W., Suzuki, Y., Yuan, X., Yoshimura, S. H., Zhang, Y., Liu, Y., Emmett, N. et al. (2014). Spatial control of proton pump H,K-ATPase docking at the apical membrane by phosphorylation-coupled ezrin-syntaxin 3 interaction. *J. Biol. Chem.* **289**, 33333-33342.

Yui, N., Okutsu, R., Sohara, E., Rai, T., Ohta, A., Noda, Y., Sasaki, S. and Uchida, S. (2009). FAPP2 is required for aquaporin-2 apical sorting at trans-Golgi network in polarized MDCK cells. *Am. J. Physiol. Cell Physiol.* **297**, C1389-C1396.

Yui, N., Lu, H. A. J., Chen, Y., Nomura, N., Bouley, R. and Brown, D. (2013). Basolateral targeting and microtubule-dependent transcytosis of the aquaporin-2 water channel. *Am. J. Physiol. Cell Physiol.* **304**, C38-C48.

Zhao, H., Shiue, H., Palkon, S., Wang, Y., Cullinan, P., Burkhardt, J. K., Musch, M. W., Chang, E. B. and Turner, J. R. (2004). Ezrin regulates NHE3 translocation and activation after Na+-glucose cotransport. *Proc. Natl. Acad. Sci. USA* **101**, 9485-9490.

Zhou, R., Cao, X., Watson, C., Miao, Y., Guo, Z., Forte, J. G. and Yao, X. (2003). Characterization of protein kinase A-mediated phosphorylation of ezrin in gastric parietal cell activation. *J. Biol. Chem.* **278**, 35651-35659.

Zhou, R., Zhu, L., Kodani, A., Hauser, P., Yao, X. and Forte, J. G. (2005). Phosphorylation of ezrin on threonine 567 produces a change in secretory phenotype and repolarizes the gastric parietal cell. *J. Cell Sci.* **118**, 4381-4391.

Zwang, N. A., Hoffert, J. D., Pisitkun, T., Moeller, H. B., Fenton, R. A. and Knepper, M. A. (2009). Identification of phosphorylation-dependent binding partners of aquaporin-2 using protein mass spectrometry. *J. Proteome Res.* **8**, 1540-1554.